**PAPER** • **OPEN ACCESS**

# Martensitic phase mechanism of ternary FeCrMn thin films influenced by the substrate rotation speeds: structural and magnetic properties

To cite this article: Nadir Kaplan and Hakan Köçkar 2024 *Phys. Scr.* **99** 105913

Physica Scripta

PAPER

# Martensitic phase mechanism of ternary FeCrMn thin films influenced by the substrate rotation speeds: structural and magnetic properties

**Nadir Kaplan and Hakan Köçkar***

Physics Department, Science and Literature Faculty, Balikesir University, 10145, Balikesir, Turkey
* Author to whom any correspondence should be addressed.

**E-mail:** nadirkaplan@baun.edu.tr **and** hkockar@balikesir.edu.tr

**Keywords:** martensitic phase, rotation speeds, FeCrMn thin films, sputtering technique, structural properties, magnetic properties

OPEN ACCESS

RECEIVED
2 July 2024

REVISED
2 August 2024

ACCEPTED FOR PUBLICATION
14 August 2024

PUBLISHED
3 September 2024



## Abstract

In order to investigate the martensitic phase mechanism of the ternary FeCrMn thin films sputtered under the effect of substrate rotation speeds, the structural and related magnetic properties were studied. A range of thin films were deposited at varying rotational speeds of 0, 15, 30, and 45 rpm on flexible amorphous polymer substrates through the use of DC magnetron sputtering. The films were 50 nm thick and were produced at 0.09 nm $s^{-1}$. The crystal structures showed that all films have a mixture of the body-centred tetragonal (bct) and tetragonal structure. The peak intensity of bct (110) martensitic $\alpha$'phase increased with the increase of the rotation speeds whereas the tetragonal (430) and (333) peaks stayed almost stable. And, the morphologic surface analysis displayed that the smooth surface turned into a rough surface with the increase of the rotation speeds. After the measurements of hysteresis loops, the films obtained by sputtering of austenitic target have ferromagnetic character with increasing saturation magnetization, $M_S$ and coercivity, $H_C$ as the substrate rotation speeds increase. With increasing rotation speeds, the increase of the $M_S$ from 148 to 242 emu $cm^{-3}$ and the rise of the $H_C$ of the films from 21 to 185 Oe might be explained by the increase of the grain sizes with the increase of % martensitic $\alpha$'phase caused by increasing rotation speeds. The ternary FeCrMn thin films exhibit increasing % martensitic $\alpha$'phase and corresponding ferromagnetic properties with increasing substrate rotation speeds. It is concluded that the nanostructured films of FeCrMn have different properties from those of their bulk counterparts under the influence of substrate rotation speeds. Therefore, the martensitic mechanism of the films can easily be controlled by changing rotation speed for potentially flexible new device applications such as spintronics, magnetic hetero-structures, magnetic separators, etc.

## 1. Introduction

Only some studies [1–7] have examined the mechanical, magnetic, and structural characteristics of the austenitic bulk FeCrMn-based stainless steels. And, the investigations looked into how their structural qualities of the bulk FeCrMn were affected by formability, phase transitions, and thermal aging [2–7]. As is well-known that the characteristics of nanostructured materials differ significantly from those of their bulk counterparts. And therefore, these differences could be advantageous in high-tech applications such as data storage devices, magnetic sensors, and micro electro-mechanical systems [8, 9].

In the vacuum methods, DC magnetron sputtering [10–15] is a viable option for producing magnetic thin films that are both reasonably low-cost and high quality. The films can be obtained by using a single target with the necessary concentration. However, the deposition parameters, such as deposition rate [10, 12, 13, 15] and rotation speeds [11, 13, 14] determine the quality and characteristics of the magnetic alloy films. In particular, it is recognized that the speed at which the substrate rotates is an effective parameter for a standard sputtering

procedure. Additionally, the flexible substrate offers a variety of options for the potential uses of the sputtered thin films in numerous industries [10–15].

In our previous studies [12–15], the ferromagnetic alloy films sputtered from iron-based commercial austenitic bulk stainless steels under the variation of the deposition parameters showed the martensitic phase of structural and related magnetic properties. From these studies, it is observed that the substrate rotation speed is the most effective parameter on the occurrence of the martensitic phases. And, martensitic FeCr films were deposited from a target made of the austenitic bulk AISI 430 stainless steel on the flexible substrate under the rotation speeds and their structural and magnetic properties were studied [13]. Also, martensitic FeCrNi films were also produced from the austenitic bulk AISI 304 stainless steel on the flexible substrate under the substrate rotation speeds [14] and their properties of structural and magnetic properties were investigated. Under the deposition rates, the FeCrMn thin films were sputtered from the austenitic bulk AISI 202 stainless steel on the flexible substrate under the effect of deposition rates [15]. The FeCrMn thin films need investigations of the influence of the substrate rotation speeds on the phase mechanism. Therefore, under study, as far as concerned, it is the first time that the martensitic mechanism of the ternary FeCrMn thin films sputtered from the commercial austenitic bulk AISI 202 stainless steel on the flexible substrate under the effect of substrate rotation speeds were investigated, and accordingly the structural and corresponding magnetic properties were presented. It is well known that nanostructure materials have distinct properties from those of their bulk equivalents [16]. Thus, under study, it is seen that the FeCrMn thin films have different structural and magnetic properties than its bulk form of commercial AISI 202 (FeCrMn) stainless steels under the changes of the substrate rotation speeds. By increasing the speeds, sputtering of the austenitic bulk FeCrMn target resulted in the thin films with the structural and magnetic properties of the increase of the martensitic $\alpha$‘ phase. These films may open up flexible new device applications, such as advancing the development of electronic and data storage devices.

## 2. Experimental

A serious of Ternary FeCrMn thin films were deposited with different substrate rotation speeds on commercially available flexible polymer substrates (acrylic acetate) using a DC magnetron sputtering system (MANTIS, Q-PREP 500, UK). As the target, a commercial bulk AISI 202 stainless steel with a diameter of 5.08 cm and a thickness of 1 mm was used. To investigate the effect of substrate rotation speed on the structural and magnetic properties of the films, the rotation speeds were chosen as 0, 15, 30, and 45 rpm with the steps of 15 rpm. The films were produced sequentially at chosen speeds while monitored in real-time with a hand-made tachometer accurate to $\pm$0.1 rpm. Before deposition, all substrates and the target source underwent a two-step cleaning process. For thorough cleaning, they were firstly bathed in distilled water followed by isopropyl alcohol, both within an ultrasonic bath (KUDOS, SK3310HP, China) for 10 min each process. After cleaning, these spontaneously stayed for drying at room temperature. Then, this cleaning process was repeated for each substrate. The target source and substrate were placed in the vacuum chamber on a DC magnetron and sample holder. Inside the vacuum chamber, the target-to-substrate distance was 12.5 cm. The vacuum chamber pressure was also dropped in the two-step evacuating process. The pressure was reduced to $5.00 \times 10^{-3}$ mbar with a rotary pump. Then, it was evacuated to a base pressure of $5.00 \times 10^{-6}$ mbar using a turbo molecular pump. Subsequently, argon gas was dispatched into the vacuum chamber to create a pure argon deposition environment in the pressure range of $3.00–4.00 \times 10^{-3}$ mbar. Throughout the sputtering process, the deposition rate was kept constant at 0.09 nm $s^{-1}$, and the environment temperature followed as $23 \pm 1$ °C. And, the total film thicknesses were monitored in real-time using a quartz crystal microbalance thickness monitor (Sycon, STM-100/MF, USA), and kept at 50 nm. After depositing, all films were stored in a glass desiccator containing silica gel to protect them from oxidation.

Following the deposition of the films, the elemental analysis was conducted using energy-dispersive x-ray spectroscopy (EDX; Bruker Quantax EDS XFlash® 6|30 system, USA). The EDX analysis focused on determining the atomic contents of only Fe, Cr and Mn within the films. To identify the crystal structures of the films were employed an x-ray diffractometer (XRD; Bruker D8 Advance diffractometer with Davinci Design for XRD$^2$ software, UK). Cu-$K_\alpha$ radiation ($\lambda = 0.15406$ nm) was utilized for the XRD analysis. XRD scans were conducted at room temperature across a $2\theta$ range of 30° to 80° with a step size of 0.005° and obtained diffraction patterns for all films. Scanning electron microscopy (SEM; ZEISS EVO LS 10, Germany) was used to examine the surface morphologies of the films. Further characterization of the film surfaces was achieved using an atomic force microscopy (AFM; NanoMagnetics Instruments Inc., hpAFM, Turkey) over a 10 $\mu$m $\times$ 10 $\mu$m scan area. The root mean square, Rms roughness and average roughness, Ra values were subsequently extracted from the AFM micrographs using Image Analyzer V4 software (developed by NanoMagnetics Instruments Inc.). Notably, the analyses of the substrates were performed without prior to any sample coating for all films. Finally, magnetic characterization was carried out using a Vibrating Sample Magnetometer (VSM, ADE TECHNOLOGIES DMS-

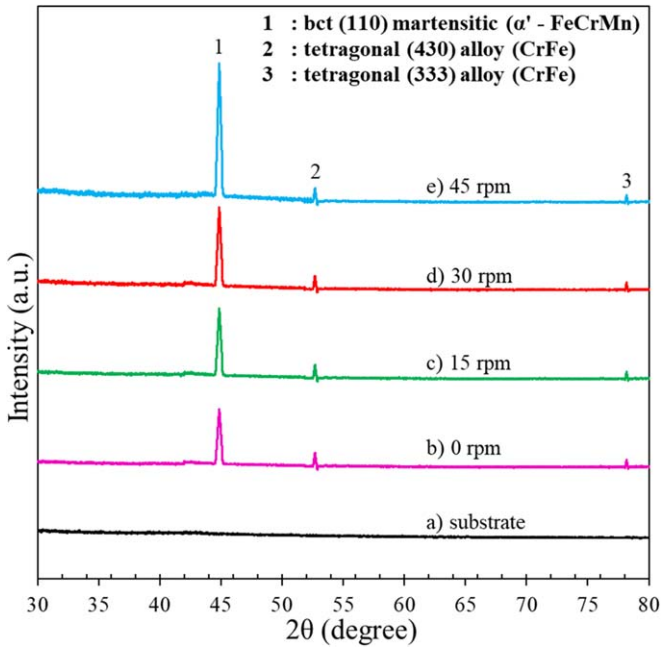


**Figure 1.** XRD patterns of (a) substrate and martensitic FeCrMn thin films sputtered at different substrate rotation speeds of (b) 0, (c) 15, (d) 30 and (e) 45 rpm.

**Table 1.** Elemental, structural and magnetic data of FeCrMn thin films sputtered at different rotation speeds of the substrate.

| | Elemental analysis | | | Crystalline properties | | Surface | | Magnetic properties | |
|---|---|---|---|---|---|---|---|---|---|
| Rotation speeds (rpm) | Fe (at. %) | Cr (at. %) | Mn (at. %) | $t_{bct(110)}$ (nm) | bct (110) martensitic phase (%) | Rms (nm) | Ra (nm) | $M_S$ (emu/cm$^3$) | $H_C$ (Oe) |
| 0 | 70.32 ± 0.02 | 15.74 ± 0.01 | 13.94 ± 0.01 | 6.9 | 84.03 | 7.99 | 7.04 | 148 | 21 |
| 15 | 71.30 ± 0.03 | 16.33 ± 0.01 | 12.37 ± 0.01 | 8.2 | 86.42 | 9.45 | 7.28 | 185 | 63 |
| 30 | 71.78 ± 0.02 | 15.89 ± 0.01 | 12.33 ± 0.01 | 10.2 | 90.12 | 9.83 | 7.35 | 217 | 131 |
| 45 | 73.30 ± 0.02 | 15.37 ± 0.01 | 11.33 ± 0.01 | 13.3 | 94.05 | 14.16 | 7.42 | 242 | 185 |

EV9, USA). Hysteresis loops were obtained at room temperature with an applied magnetic field of ±20 kOe intervals in 1 Oe steps. To avoid the shape anisotropy, the films were circularly prepared.

## 3. Results and discussion

Based on EDX measurements, elemental analysis findings of the FeCrMn thin films were obtained and are shown in table 1. The atomic composition of commercial bulk AISI 202 stainless steels were 76.9% Fe, 12.1% Cr, and 10.0% Mn with 0.9% additional elements of Cu, Ni, Co, and V [15]. A small deviation exists between the target contents and the atomic percentage of Fe, Cr, and Mn in the films. All of the Fe levels of the films were lower than that of the target material but their Cr and Mn contents were higher. Since Fe has a rather high melting point, it is known to sputter it hard [17]. This is most likely the case. However, the variation of the substrate speeds causes a change in the atomic fraction of the elements in the films. When the rotation speed increases from 0 to 45 rpm, the atomic percentage of Fe in the film increases from 70.32 ± 0.02% to 73.30 ± 0.02% and the Mn in the films slightly decreases from 13.94 ± 0.01% to 11.33 ± 0.01%. And, the atomic percentage of Cr stays between 15.37 ± 0.01% and 16.33 ± 0.01%.

Figures 1(a)–(e) shows the XRD patterns of the substrate and FeCrMn films sputtered at different rotation speeds. Due to the amorphous structure of the substrate, no peak is seen; see figure 1(a). As shown in figures 1(b)–(e), three distinct peaks emerged, designated as 1, 2 and 3, respectively: the body-centred tetragonal bct (110) martensitic $\alpha$'-phase, tetragonal (430), and tetragonal (333) [15]. As the rotation speeds in figures 1(b)–(e) increase, the bct(110) martensitic $\alpha$'-phase increased while the tetragonal (430) and (333) phases almost

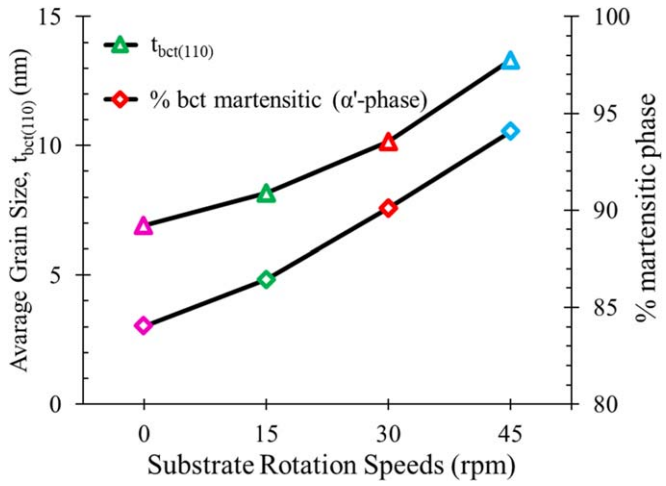


**Figure 2.** Plots of average grain size, $t_{bct(110)}$ and % martensitic phase against the substrate rotation speeds of the films.

unchanged. By calculating the ratio of all peaks throughout the area of the bct (110) plane, the volume fraction of the martensite percentage of the bct (110) peak was determined as calculated from the [17]. For the rotation speeds of 0, 15, 30, and 45 rpm, respectively, the percentages are found to be 84.03, 86.42, 90.12 and 94.05%, as indicated in table 1. Using the full width at half maximum (FWHM) value of the bct(110) peak, the Scherrer formula [18] was used to calculate the average grain size, $t_{bct}(110)$, which is shown in table 1. The table illustrates that the films sputtered at the rotation speeds of 0, 15, 30, and 45 rpm yielded the $t_{bct}(110)$ values of approximately 6.9, 8.2, 10.2 and 13.3 nm, respectively,. It has been noted that when the rotation speed increases, the $t_{bct}(110)$ values of the films increases. Plotting the average grain size, $t_{bct}(110)$ and martensite phase percentage against rotation speeds produced the results shown in figure 2. As seen in the figure, the $t_{bct}(110)$ values and martensitic phase percentage increased with the increase of the rotation speeds. Nanostructure materials are known to possess different characteristics from their bulk counterparts [16]. Hence, it is demonstrated in this study that, as substrate rotation speeds rise, the structural characteristics of FeCrMn in thin film form diverge from those of the bulk form in bulk AISI 202 (FeCrMn) stainless steels. It should also be noted that the $t_{bct}(110)$ values under study are also slightly higher than the thin film form of FeCrMn study due to the effect of using different production parameter from the study [15]. The production parameters affect the properties of the thin films [10–15] and some of them [12–15] displayed that the films have martensitic properties. And therefore, the main aim of the study was to investigate the effect of the variations of the substrate rotation speeds on the martensitic phase mechanism of the FeCrMn thin films. The calculations from the peak intensities of bct (110) martensitic $\alpha$'phase of the thin films showed that the fraction of martensitic phase increased as the substrate rotation speed increased This means that when rotation speeds increased, the martensitic phase percentage is responsible for the increase in grain sizes. Besides, using the Bragg formula [18], the interplanar spacing for bct (110) planes, $d_{bct(110)}$ was determined to be around 0.2019 regardless of the rotation speeds. For lattice constant for bct (110) planes, $a_{bct}$ values, they were calculated as approximately 0.2895 nm. Based on the calculations, the $a_{bct}$ values lie between those of bulk Fe ($a_{Fe} = 0.2866$ nm) and Cr ($a_{Cr} = 0.2979$ nm) and are close to bulk Mn ($a_{Mn} = 0.3782$ nm) [18–20]. It is obtained from the XRD patterns that the ternary FeCrMn films displayed the increase of martensitic phase percentage with increasing $t_{bct}(110)$ values caused by the increase of the substrate rotation speeds It is well known that materials having nanostructures have unique properties different from their bulk counterparts [16]. For this reason, due to the sputtering of bulk AISI 202 (FeCrMn) stainless steels under the variations of substrate rotation speeds, it is thought that the austenite phase is transformed to martensitic FeCrMn thin films.

SEM images of the substrate and the films sputtered at various substrate rotation speeds were displayed in figure 3. The smooth and deformation-free surface of the substrate is visible in figure 3(a). As seen in figure 3(b), the film sputtered at the stationary (0 rpm) case has a comparatively flat surface. And, in figure 3(c), the film sputtered at 15 rpm has a comparatively homogeneous surface with small narrow strip-like areas in the image. A work concerning sputtered FeCrMn films [15] has SEM images that clearly display areas with varying crystal structures depending on deposition rates. In our study, images captured by SEM revealed morphological results that pointed to the locations of distinct crystal formations. Depending on the contrast, the image in figure 3(d) displays separate regions with dark and light sides at the rotation speed of 30 rpm. The darker and lighter areas in the film deposited at 45 rpm of figure 3(e) are easily distinguishable from one another, which may indicate a difference in the crystal structure. The XRD patterns of the films appear to be compatible with the SEM images,

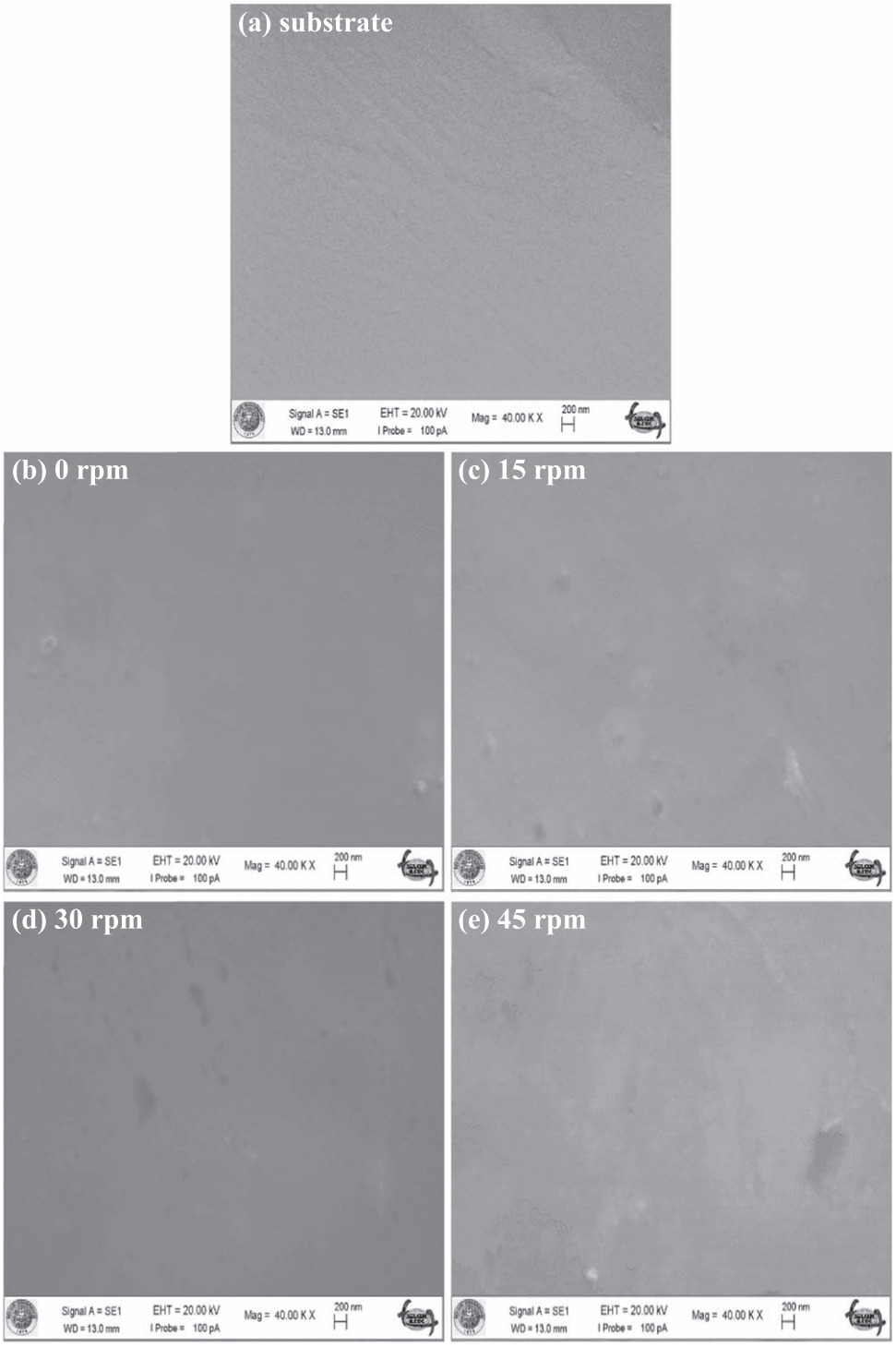


**Figure 3.** SEM images displaying the (a) substrate and martensitic FeCrMn thin films sputtered at (b) 0, (c) 15, (d) 30 and (e) 45 rpm of the substrate rotation speeds.

displaying a mixed body-centred tetragonal bct (110) martensitic $\alpha$'-phase, tetragonal (430), and tetragonal (333) structure. Although studies [21–23] have shown that a comparatively higher iron content in the films may be the cause of the increased surface inhomogeneity, under study this may have come from the increase of martensitic phase percentage under the increase of the rotation speeds. In order to examine the compositional homogeneity of the films, local EDX analysis was also carried out on the films. It was found that all films have a consistent composition throughout their surface (data not shown). It is observed that the smooth surface of the films turned into the inhomogeneity shaped morphology with the rise of the martensitic phase percentage caused by the increase of the substrate rotation speeds.

AFM image of the substrate was taken and shown in figure 4(a). Figures 4(b)–(e) presents the AFM images that were acquired from the films sputtered at substrate rotation speeds of 0, 15, 30, and 45 rpm, respectively.

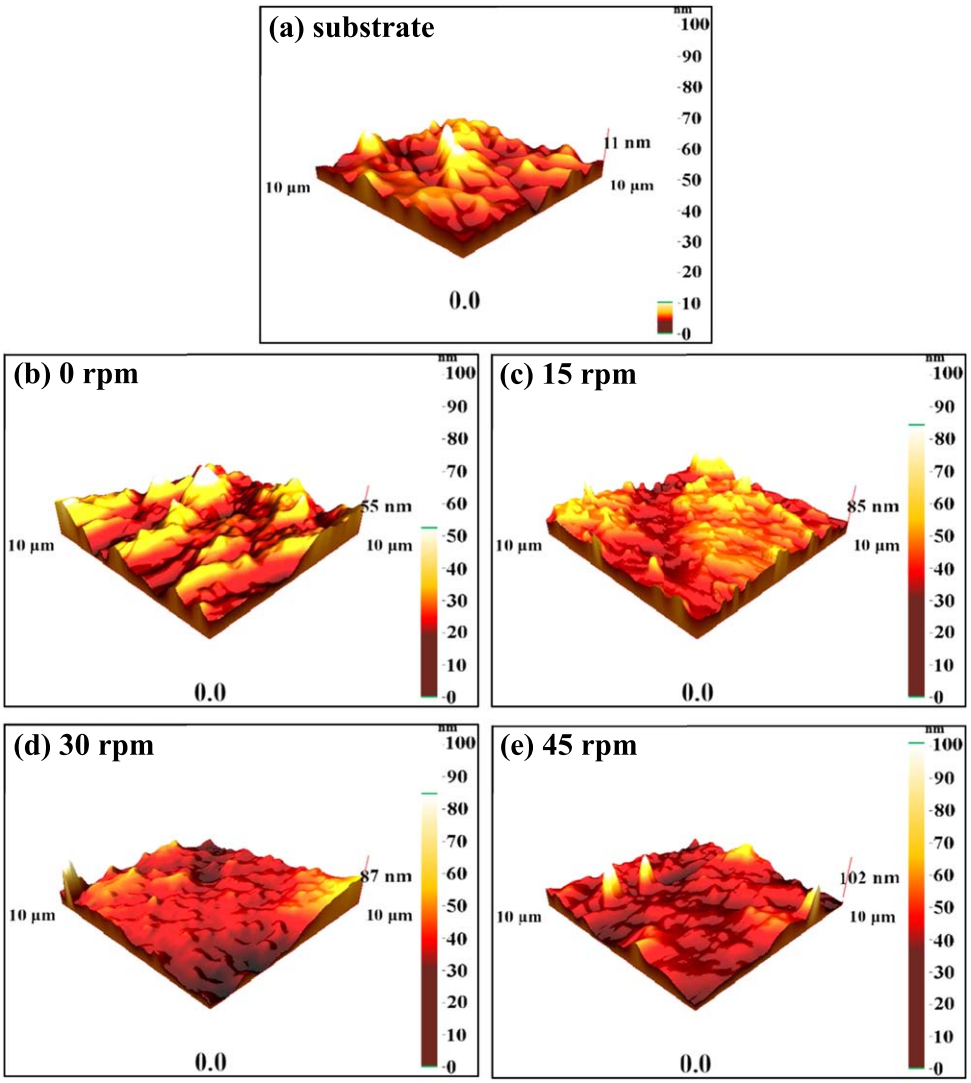


**Figure 4.** AFM images demonstrating (a) substrate and martensitic FeCrMn thin films sputtered at (b) 0, (c) 15, (d) 30 and (e) 45 rpm of the substrate rotation speeds.

The surfaces are described using the root mean square, Rms and the average roughness, Ra acquired from AFM images. In table 1, these values are displayed. According to calculations, the Rms values, which show the average of surface roughness, for the films increased from 7.99 to 14.16 nm with the increase of rotation speeds from 0 to 45 rpm. And, the Ra values, increased from 7.04 to 7.42 nm for the films sputtered from 0 to 45 rpm. For the FeCrNi films sputtered from austenitic AISI 304 stainless steels [14], the order of these values was found to be vice versa to the current study under the increase of substrate rotation speeds. Under study, it is possible to draw the conclusion that raising the rotation speed could raise the Ra and Rms values of the FeCrMn films sputtered from austenitic AISI 202 stainless steels. It was also discovered that when the martensitic phase percentage increased under the speed of the substrate rotation, the homogeneous film surface transferred into a rougher structure, as seen in AFM images in figure 4. It is evident that the SEM and AFM observed surface properties of the films were consistent under study.

For magnetic analysis of the FeCrMn thin films, the hysteresis loops of the films were plotted at ±3 kOe as displayed in figure 5. The data obtained from the loops are shown in table 1. The magnetic measurement of austenitic bulk AISI 202 stainless steels, in contrast to prior investigations of showing paramagnetic behaviour [5–7, 24], exhibits paramagnetic and weak ferromagnetic components in our previous study [15]. After sputtering of bulk AISI 202 stainless steels under the increase of the substrate rotation speeds, the ferromagnetic nature of the FeCrMn thin films occurred due to the martensitic phase as obtained from XRD measurements, see table 1, figure1 and figure 5. With the increase of rotation speeds, the saturation magnetisation, $M_S$ of the films increased from 148 to 242 emu $cm^{-3}$ and, the coercivity, $H_C$ values of the films increases from 21 to 185 Oe. In figure 6 and figure 7, the variations of $M_S$ and $H_C$ values against % martensitic phase under the substrate rotation speeds were plotted, respectively. Mn is paramagnetic and Cr is antiferromagnetic while Fe is

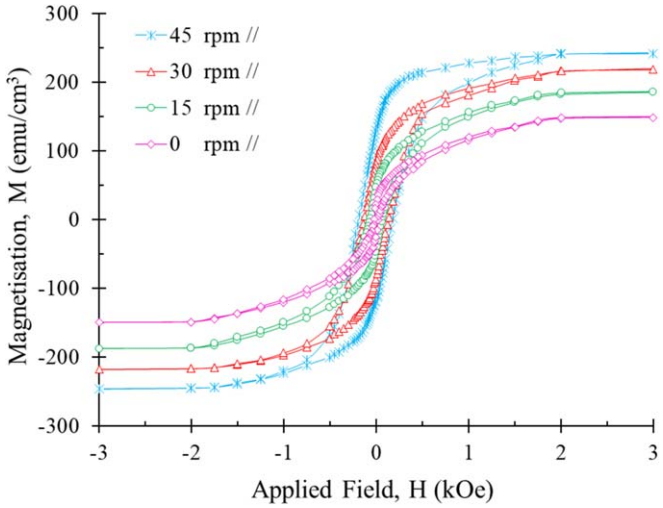


**Figure 5.** Magnetic hysteresis loops of martensitic FeCrMn thin films at the substrate rotation speeds of 0, 15, 30 and 45 rpm are plotted at ± 3 kOe.

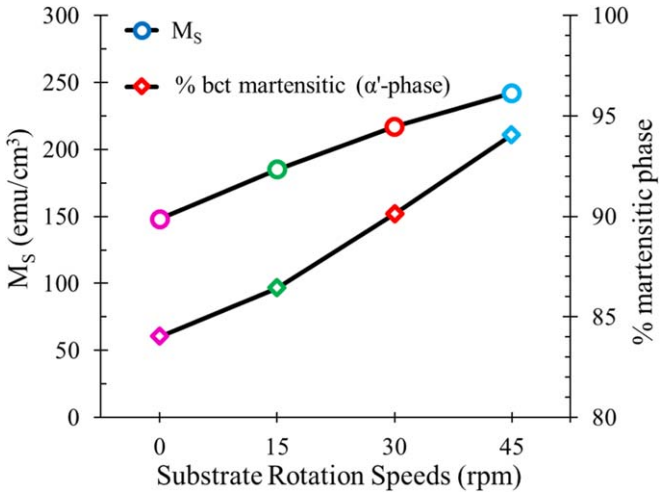


**Figure 6.** The saturation magnetisation, $M_S$ and % martensitic phase against the substrate rotation speeds of 0, 15, 30 and 45 rpm.

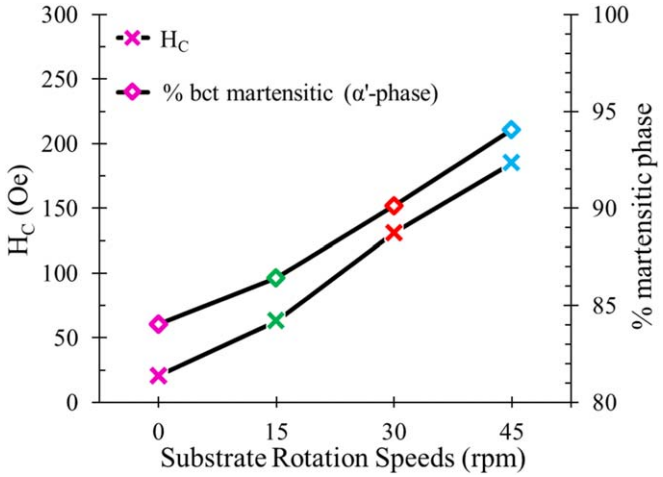


**Figure 7.** Plot of the coercivity, $H_C$ and % martensite versus the substrate rotation speeds of 0, 15, 30 and 45 rpm.

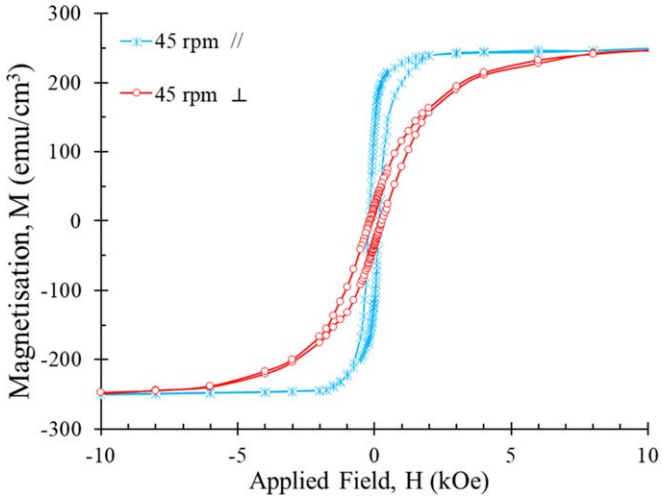


**Figure 8.** The parallel and perpendicular hysteresis loops of the martensitic FeCrMn thin film sputtered at 45 rpm are plotted at ± 10 kOe.

ferromagnetic at room temperature in nature [8]. The relationships between these three elements might be ignorable since they have different magnetic characteristics. There is only Fe as an element to consider for the change of the magnetisation. As seen in figure 6, the main contribution to the $M_S$ values of the films may come from the increase of martensitic percentage since the rise in Fe content (around 3%) may be insufficient to explain the increase of $M_S$ values (approximately 39%) under increasing rotation speeds. As in the investigations [14, 15], although the slight variations of iron content in the films are expected to be the cause of the $M_S$ values, the reason under study is thought to be coming from the martensitic phase mechanism of the films. In the case of the $H_C$ values, it increased with the increase of the $t_{bct}(110)$ values as the martensitic percentage increased, which caused by the increase of the rotation speeds. In figure 6 and figure 7, the % martensitic phase steadily increases and strengthens the ferromagnetic character with the increase of substrate rotation speeds. Therefore, it can be said that when rotation speeds increased, the martensitic phase percentage which is responsible for the rise in grain size, caused an increase in the $M_S$ and $H_C$ values. Besides, figure 8 provides an example of the parallel and perpendicular hysteresis loops of the film sputtered at 45 rpm rotation speed. Perpendicular loop refers to exactly 90 degrees to the film plane. Because of the shape anisotropy, the magnetic easy-axis is observed to be in the film plane. Similar results of the loops for the in-plane easy-axis were seen in the remaining films of the investigation.

## 4. Conclusions

Under varying substrate rotation speeds, martensitic FeCrMn thin films sputtered onto a flexible amorphous polymer substrate from a single target composed of commercial austenitic bulk AISI 202 stainless steels using a DC magnetron sputtering technique were examined. The compositional analyses of the films revealed that when rotation speeds increased, the Fe content of the films rose, and their Mn content fell. And, x-ray diffraction technique displayed that the peak intensity of bct (110) martensitic $\alpha$'phase increased with the increase of the rotation speeds whereas the tetragonal (430) and (333) peaks stayed nearly constant. With a further investigation, grain size and martensitic percentage of the films increased with increasing rotation speeds. Also, the morphological analysis of the film surfaces, performed by a scanning electron microscope and atomic force microscope, presented that the homogeneous surfaces of the films changed into rough structure with increasing rotation speeds. In the case of magnetic analysis, the increase of the ferromagnetic nature of the FeCrMn thin films were obtained under the increase of the rotation speeds. And, the increase of the saturation magnetisation from 148 to 242 emu $cm^{-3}$ and the coercivity of the films from 21 to 185 Oe may be explained by the increase of the grain sizes with the increase of the martensitic phase percentage caused by increasing rotation speeds. Therefore, the martensitic phase occurred in ternary FeCrMn thin films can be controlled by changing substrate rotation speeds for potential data storage and micro electric-electronic devices on flexible substrates.

## Acknowledgments

This study was funded by the Balikesir University under grants no BAP 2016/132 and 2022/068 and also by the State Planning Organization/Turkiye under grant no 2005K120170 for DC Magnetron Sputtering and VSM systems. The authors thank to Dr H Kuru from Balikesir University, Turkiye for VSM measurements and also Dr A Karpuz from Karamanoglu Mehmetbey University, Turkiye for his help of the film measurements. And, the authors are grateful to Selcuk University, İLTEK, Turkiye for SEM and EDX analysis, Karamanoglu Mehmetbey University, BILTEM, Turkiye for XRD measurements.

## Data availability statement

All data that support the findings of this study are included within the article (and any supplementary files).

## Author contributions

Nadir Kaplan produced the films according to the experimental plan and prepared the table and figures, and also interpret the most analyses of the results. Hakan Köçkar directed the study and contributed to the measurements and interpretation of all results, and wrote the article.

## Conflict of interest

The authors declare that they have no conflict of interest.

## ORCID iDs

Nadir Kaplan https://orcid.org/0000-0002-2471-1179
Hakan Köçkar https://orcid.org/0000-0002-4862-0490

## References

[1] Al-Zoubi N, Li X, Schönecker S, Johansson B and Vitos L 2014 Influence of manganese on the bulk properties of Fe-Cr-Mn alloys: a first-principles study *Phys. Scr.* **89** 125702
[2] Vigneshvar V S and Sudhakaran R 2014 A review on performance improvement in the weldment regions of chromium manganese stainless steels (AISI 202 SS) *I International Journal for Research in Applied Science & Engineering Technology, (IJRASET)* **2** 416–9
[3] Shukla S, Patil A P, Kawale A P, Singh S K and Thombre M A 2021 Effect of thermal ageing and deformation on microstructural evolution of 304 and 202 grade steel *Materials Today: Proceedings* **38** 3238–45
[4] Panov D, Kudryavtsev E, Chernichenko R, Smirnov A, Stepanov N, Simonov Y, Zherebtsov S and Salishchev G 2021 Mechanisms of the reverse martensite-to-austenite transformation in a metastable austenitic stainless steel *J. Met.* **11** 599
[5] Du Toit M and Steyn H G 2012 Comparing the formability of AISI 304 and AISI 202 stainless steels *J. Mater. Eng. Perform.* **21** 1491–5
[6] Schneider T, Acet M, Wassermann E F and Pepperhoff W 1991 Magnetism and segregation in Fe-Cr-Mn *J. Appl. Phys.* **70** 6559–61
[7] Igata N, Aoyama H, Kanja Y and Habara Y 1996 High damping Fe-Cr-Mn alloy *Le Journal de Physique IV* **6** **791**
[8] Jiles D 2015 *Introduction to magnetism and magnetic materials* 3rd Ed. (CRC press) 76
[9] Shi D and Hongchen G 2008 Nanostructured magnetic materials and their applications *J. Nanomater.* **2008** 1–2
[10] Köçkar H *et al* 2019 Easy controlled properties of quaternary FeNiCrCd thin films deposited from a single dc magnetron sputtering under the influence of deposition rate *Journal of Superconductivity and Novel Magnestism* **32** 3535–40
[11] Köçkar H and Şentürk Ö 2019 Rotation speed induced properties of quaternary FeNiCrCd thin films easy-prepared from a single magnetron sputtering *Optoelectronics and Advanced Materials - Rapid Communications* **13** 620–3
[12] Kaplan N, Köçkar H, Karpuz A, Kuru H and Uçkun M 2019 Ternary FeCrNi martensitic thin films sputtered on a flexible substrate from a single AISI 304 austenitic stainless steel source: effect of deposition rate on structural and magnetic properties *J. Magn. Magn. Mater.* **476** 597–603
[13] Köçkar H, Kaplan N, Karpuz A, Kuru H and Kaya B 2019 Characterizations of binary FeCr (AISI 430) thin films deposited from a single magnetron sputtering under easy controllable deposition parameters *J. Supercond. Novel Magn.* **32** 2457–65
[14] Köçkar H and Kaplan N 2020 Single crystal martensitic phase of structural properties-related magnetic behaviour of FeCrNi thin films: in-plane magnetic anisotropy under different substrate rotation speeds *J. Mater. Sci., Mater. Electron.* **31** 12823–9
[15] Köçkar H, Kaplan N and Karaagac O 2023 Martensitic ternary FeCrMn thin films sputtered from austenitic AISI 202 stainless steel target: phase transition and corresponding magnetic properties under the influence of deposition rate *J. Magn. Magn. Mater.* **587** 171352
[16] Logothetidis S (ed) 2012 *Nanostructured materials and their applications* (Springer Science & Business Media)
[17] Liao Y 2007 *Practical Electron Microscopy and Database - An Online Book* Second Edition http://globalsino.com/EM/ (accessed 10 Jun 2024)
[18] Cullity B D and Stock S R 2014 *Elements of X-ray Diffraction* (Pearson Education Limited) p 290, p 413 92–7
[19] Strack G *et al* 2022 Magnetic nanoarrays on flexible substrates *MRS Adv.* **7** 410–4
[20] Williamson G K and ve Hall W H 1953 X-Ray line broadening from filed aluminium and wolfram *Acta Metall.* **1** 22–31

[21] Razumovskiy V I, Hahn C, Lukas M and Romaner L 2019 *Ab Initio* study of elastic and mechanical properties in FeCrMn alloys *Materials* **12** 1129
[22] Gich M, Shafranovsky E A, Roig A, Slawska-Waniewska A, Racka K, Casas L, Petrov Y Y, Molins E and Thomas M F 2005 Aerosol nanoparticles in the Fe1−xCrx system: room-temperature stabilization of the $\sigma$ phase and $\sigma \rightarrow \alpha$-phase transformation *J. Appl. Phys.* **98** 024303
[23] De A K, Murdock D C, Mataya M C, Speer J G and Matlock D K 2004 Quantitative measurement of deformation-induced martensite in 304 stainless steel by X-ray diffraction *Scr. Mater.* **50** 1445–9
[24] Mészáros I and János P 2005 Magnetic investigation of the effect of $\alpha'$-martensite on the properties of austenitic stainless steel *J. Mater. Process. Technol.* **161** 162–8